Research Article

Rehab M. El-Shiekh* and Mahmoud Gaballah

Solitary chirp pulses and soliton control for variable coefficients cubic–quintic nonlinear Schrödinger equation in nonuniform management system

https://doi.org/10.1515/phys-2025-0147
received December 28, 2024; accepted March 11, 2025

Abstract: This study investigates the variable coefficient cubic–quintic nonlinear Schrödinger equation, which models the propagation of ultrashort femtosecond pulses in optical fibers and three-body recombination losses in Bose–Einstein condensates. Using a mapping technique combined with an extended chirp wave transformation, 20 chirp wave solutions were derived, including bright and dark solitons, kink waves, periodic and singular waves. These solutions encompass previously reported results and introduce novel ones. Three-dimensional plots illustrate the soliton and kink chirp wave solutions for both constant and exponentially varying group velocity dispersion (GVD) and Raman effect parameters. Analysis reveals that the sign of the Raman effect parameter influences the soliton type, yielding bright solitons for positive values and dark solitons for negative values. Furthermore, both GVD and Raman effect significantly impact the wave shape, inducing oscillations in the case of exponentially distributed fiber. The stability of the soliton wave solution is also analyzed. These diverse wave profiles have potential applications in nonlinear optics and plasma physics.

Keywords: variable coefficients cubic–quintic nonlinear Schrödinger equation, mapping method, stability analysis, chirp waves

*** Corresponding author: Rehab M. El-Shiekh,** Department of Business Administration, College of Business Administration in Majmaah, Majmaah University, Al Majmaah 11952, Saudi Arabia,
e-mail: r.abdelhaim@mu.edu.sa
Mahmoud Gaballah: Department of Physics, College of Science at Al-Zulfi, Majmaah University, Al Majmaah 11952, Saudi Arabia; Geomagnetic and Geoelectric Department, National Research Institute of Astronomy and Geophysics (NRIAG), 11421 Helwan, Cairo, Egypt,
e-mail: m.abdelmawgoud@mu.edu.sa

1 Introduction

The variable coefficient nonlinear Schrödinger (VCNLS) equation is a generalization of the nonlinear Schrödinger (NLS) equation that allows for the coefficients to vary with position and time. This makes it a more versatile equation for modeling a wider range of physical phenomena. It can be used to describe the propagation of light pulses through optical fibers and other nonlinear materials with varying properties [1], the behavior of ultracold atoms trapped in inhomogeneous potentials [2], the dynamics of plasma waves in nonuniform plasmas [3], and the propagation of sound waves through nonlinear materials with variable properties [4]. This equation, which generalizes the NLS equation by allowing for variable coefficients, is essential for studying the complex interactions between waves and their environments [4–10]. The VCNLS equation can be written as:

$$i\psi_x + \alpha(x)\psi_{tt} + \beta(x)|\psi|^2\psi = 0, \tag{1}$$

where ψ is the complex-valued wave function that can represent the envelope of an electric field, t is the time, x is the distance, $\alpha(x)$ is the variable group velocity dispersion (GVD) coefficient, and $\beta(x)$ is the variable nonlinear in optics. The amplitude $|\psi|^2$ denotes the intensity or optical power. The linear terms in the VCNLS equation represent the dispersion of the wave, while the nonlinear term represents the interaction between the wave and itself. The variable coefficients allow for the modeling of inhomogeneous media and time-dependent effects [1–10].

One of the very important VCNLS equations is the variable coefficients cubic–quintic nonlinear Schrödinger (VCQNLS) equation, which can be used to describe the ultrashort optical pulses obtained by increasing the intensity of the incident light field in the presence of higher-order nonlinear terms, like self-steepening and self-frequency shift [11,12]. Additionally, the existence of quintic nonlinearity is vital for studying three-

body recombination losses in the circumstances of Bose–Einstein condensates [12–17]. Therefore, in this work, we are going to study the VCQNLS, which is given by

$$i\psi_x + \alpha(x)\psi_{tt} + \beta(x)|\psi|^2\psi + \gamma(x)|\psi|^4\psi + i\delta(x)(|\psi|^2)_t\psi = 0. \quad (2)$$

By comparison between Eqs (1) and (2), we can see that there are two additional terms, the quintic term ($|\psi|^4\psi$) corresponding to three-body interatomic interactions with coefficient, $\gamma(x)$, representing the non-Kerr nonlinearity in optics, which allows for a more accurate description of the nonlinear effects in non-Kerr media. This is particularly important for ultrashort optical pulses, where the intensity can be very high [11,12]. While $\delta(x)$ accounts for the Raman effect, which causes self-frequency shift. Eq. (2), where α, β, γ, and δ are constants, was originally discovered by Kundu while he was studying gauge connections between generalized Landau–Lifshitz and higher-order NLS systems, so it is called in many context Kundu Eckhaus (KE) equation [12–24]. This equation accurately models the propagation of ultrashort optical pulses in nonlinear optics and analyzes the stability of Stokes wave in weak nonlinear dispersive matter waves and many recent studies were done for the constant KE equation [12–24].

The VCQNLS Eq. (2) was investigated by Wang *et al.* [11] using a similarity transformation. They converted it into the KE equation with constant coefficients and employed known solutions from the literature to derive one and two soliton solutions under specific conditions on the variable coefficients. Subsequently, Xie and Yan [12] utilized the bilinear form to construct one and two soliton solutions, albeit under different relationships between the variable coefficients.

However, the mentioned research works focus on soliton wave-type solutions, and to the best of our knowledge, other wave solutions like kink and periodic types have not been obtained before. From our review on constant coefficients version of Eq. (2) [12–24], we have found that chirp wave solution was obtained, and this inspired us to generalize the chirp wave transformation to be dependent on variable functions and combined it with the mapping method [26–28] to be able to find different chirp wave solutions for Eq. (2). Moreover, it was the first time the mapping method was applied to nonlinear partial differential equations (NPDEs) with variable coefficients like the VCQNLS equation.

This study is devoted to five sections, Section 1 gives the introduction and literature review, Section 2 describes methodology, in Section 3, the application of the methodology and novel wave solutions are given, then in Section 4, physical applications containing dynamic behavior of some chirp wave solutions and its stability are given, and, finally, conclusion and important remarks are given in Section 5.

2 Methodology

In recent times, numerous novel techniques have been explored for solving NPDEs [29–31], then mean focusing has been done on extending and generalizing these methodologies to address NPDEs with variable coefficients [27–31]. One of those techniques is the mapping method introduced by Zayed *et al.* [26–28], it stands out as one such technique with extensive applications in NPDEs featuring constant coefficients. However, its generalization to solve NPDEs with variable coefficients is yet to be realized. Based on our literature review of the constant KE equation [21–25], we have devised a generalization of the traveling wave transformation presented therein. This generalization enables us to derive chirp solitary wave for the VCQNLS, as follows:

(1) If a complex NPDE defined as

$$P(x, t, \psi, \psi_x, \psi_t, \psi_{xx}, \ldots) = 0, \quad (3)$$

where x, t are the independent variables and ψ is the dependent variable. To reduce Eq. (3) to a nonlinear ordinary differential equation (NODE), use the following extended traveling wave transformation [21–25]:

$$\psi(x, t) = P(\eta)e^{i(r(x)-qt+f(\eta))}, \quad (4)$$

where $\eta(x, t) = t - kx$, $P(\eta)$ is the amplitude real function, $f(\eta)$ is also a real function representing the nonlinear phase and $k = \frac{1}{v}$ is the inverse velocity. Moreover, $r(x)$ is an arbitrary function of x and q is a real constant representing the frequency shift.

(2) By using transformation (4) in Eq. (3), it transformed to an NODE in $P(\eta)$ as

$$\Omega(P, P', P'', \ldots) = 0, \quad (5)$$

(3) If

$$P(\eta) = \sum_{j=0}^{j=2M} B_j F^j(\eta), \quad (6)$$

where $F(\eta)$ is given from the solution of the first-order NODE equation

$$F'^2(\eta) = aF^2(\eta) + \frac{b}{2}F^4(\eta) + \frac{c}{3}F^6(\eta) + d. \quad (7)$$

The positive real number M can be determined by balancing the linear and nonlinear terms in Eq. (3). Eq. (7) has known solutions with established relationships between the real constants a, b, c, and d. Furthermore, the constants B_j can be calculated by substituting Eqs (6) and (7) in

Eq. (5), equating the coefficients of different powers of F to zero, and solving the resulting algebraic system using the Maple program.

3 Novel solitary waves for the VCQNLS

To derive solitary and periodic chirp wave solutions, we must employ the transformation defined by Eq. (4) to convert the VCQNLS into an NODE. Subsequently, we separate the NODE into its real and imaginary components as follows:

$$\alpha(x)P'' + [(kf' - r'(x)) - \alpha(f' - q)^2]P + \beta(x)P^3 + \gamma(x)P^5 = 0, \tag{8}$$

$$[2\alpha(x)(f' - q) - k]P' + 2\delta(x)P^2P' + \alpha(x)f''P = 0. \tag{9}$$

By integrating Eq. (9) for η variable, assuming a zero integration constant, we obtain the following equation:

$$f' = \frac{k}{2\alpha(x)} + q - \frac{\delta(x)}{2\alpha(x)}P^2. \tag{10}$$

Substituting Eq. (10) in Eq. (8) yields the following NODE:

$$\alpha(x)P'' + \left[k\left(\frac{k}{4\alpha(x)} + q\right) - r'(x)\right]P + \beta(x)P^3 + \left(\gamma(x) - \frac{\delta^2}{4\alpha(x)}\right)P^5 = 0. \tag{11}$$

Divide all terms of Eq. (11) by $\alpha(x)$

$$P'' + \frac{1}{\alpha(x)}\left[k\left(\frac{k}{4\alpha(x)} + q\right) - r'(x)\right]P + \frac{\beta(x)}{\alpha(x)}P^3 + \frac{1}{\alpha(x)}\left(\gamma(x) - \frac{\delta^2}{4\alpha(x)}\right)P^5 = 0. \tag{12}$$

Then, assume that the variable coefficients are nonzero constants $C_1 = \frac{1}{\alpha(x)}\left[k\left(\frac{k}{4\alpha(x)} + q\right) - r'(x)\right]$, $C_2 = \frac{\beta(x)}{\alpha(x)}$, $C_3 = \frac{1}{\alpha(x)}(\gamma(x) - \frac{\delta^2(x)}{4\alpha(x)})$. Based on the aforementioned analysis, the following integrability relations emerge:

$$r(x) = \int\left[\left(\frac{k}{4\alpha(x)} + q\right)k - \alpha(x)C_1\right]dx, \quad \beta(x) = C_2\alpha(x), \gamma(x) = C_3\alpha(x) + \frac{\delta^2(x)}{4\alpha(x)}. \tag{13}$$

We can see that all variable parameters depend on only two variables $\alpha(x)$, the GVD coefficient, and $\delta(x)$, the self-frequency shift or Raman effect. Now, Eq. (12) becomes

$$P'' + C_1P + C_2P^3 + C_3P^5 = 0. \tag{14}$$

From Eq. (6), we should first determine the value of M from the balance between the terms P'' and P^5, which we have obtained as $M = \frac{1}{2}$. Therefore, (14) has a solution in the form

$$P = B_0 + B_1F, \tag{15}$$

where B_0 and B_1 are arbitrary constants. By substituting Eq. (15) in Eq. (14) and applying Riccati Eq. (7), we obtain a function on F^i, $i = 0, 1, \ldots, 5$. Setting all coefficients of this function to zero yields the following equations:

The coeff. of F^5: $C_3B_1^5 + cB_1 = 0$,
The coeff. of F^4: $5C_3B_0B_1^4 = 0$,
The coeff. of F^3 : $B_1b + C_2B_1^3 + 10C_3B_0^2B_1^3 = 0$,
The coeff. of F^2 : $3C_2B_0B_1^2 + 10C_3B_0^3B_1^2 = 0$,
The coeff. of F : $B_1a + C_1B_1 + 3C_2B_0^2B_1 + 5C_3B_0^4B_1 = 0$,
The coeff. of F^0 : $C_1B_0 + C_2B_0^3 + C_3B_0^5 = 0$.

Upon solving the preceding system, we arrive at the following values:

$$A_0 = 0, A_1 = \pm\sqrt{-\frac{b}{C_2}}, a = C_1, c = -\frac{b^2C_3}{C_2^2}. \tag{16}$$

Using the 20 values of F from previous literature [26–28], we obtain the following solutions to the VCQNLS equation.

$$P_1 = \pm 4\sqrt{-\frac{b}{C_2}}\left(\frac{C_1\tanh^2\left(\varepsilon\sqrt{\frac{C_1}{3}}\eta\right)}{3b\left(3 + \tanh^2\left(\varepsilon\sqrt{\frac{C_1}{3}}\eta\right)\right)}\right)^{\frac{1}{2}}, \quad C_1 > 0, b > 0, C_3 = \frac{3C_2^2}{16C_1}, \tag{17}$$

$$P_2 = \pm\sqrt{-\frac{b}{C_2}}\left(\frac{2C_1}{b}(1 + \tanh(\varepsilon\sqrt{-C_1}\eta))\right)^{\frac{1}{2}}, C_1 < 0, \quad C_3 = \frac{3C_2^2}{16C_1}, d = 0, \tag{18}$$

$$P_3 = \pm 4\sqrt{-\frac{b}{C_2}}\left(\frac{C_1\coth^2\left(\varepsilon\sqrt{\frac{C_1}{3}}\eta\right)}{3b\left(3 + \coth^2\left(\varepsilon\sqrt{\frac{C_1}{3}}\eta\right)\right)}\right)^{\frac{1}{2}}, \quad C_1 > 0, b > 0, C_3 = \frac{3C_2^2}{16C_1}, \tag{19}$$

$$P_4 = \pm 4\sqrt{-\frac{b}{C_2}}\left(\frac{-C_1\tan^2\left(\varepsilon\sqrt{\frac{-C_1}{3}}\eta\right)}{3b\left(3 - \tan^2\left(\varepsilon\sqrt{\frac{-C_1}{3}}\eta\right)\right)}\right)^{\frac{1}{2}}, \quad C_1 < 0, b > 0, C_3 = \frac{3C_2^2}{16C_1}, \tag{20}$$

$$P_5 = \pm 4\sqrt{-\frac{b}{C_2}}\left(\frac{-C_1\cot^2\left(\varepsilon\sqrt{\frac{-C_1}{3}}\eta\right)}{3b\left(3-\cot^2\left(\varepsilon\sqrt{\frac{-C_1}{3}}\eta\right)\right)}\right)^{\frac{1}{2}}, \quad C_1 < 0, b > 0, C_3 = \frac{3C_2^2}{16C_1}, \tag{21}$$

$$P_6 = \pm\sqrt{-\frac{b}{C_2}}\left(\frac{2C_1}{b}(1+\coth(\varepsilon\sqrt{-C_1}\eta))\right)^{\frac{1}{2}}, \quad C_1 < 0, C_3 = \frac{3C_2^2}{16C_1}, d = 0, \tag{22}$$

$$P_7 = \pm\sqrt{-\frac{b}{C_2}}\left(\frac{6C_1b\operatorname{sech}^2(\sqrt{-C_1}\eta)}{3b^2+4C_1c(1+\varepsilon\tanh(\sqrt{-C_1}\eta))^2}\right)^{\frac{1}{2}}, \quad C_1 < 0, C_3 = \frac{-C_2^2c}{b^2}, d = 0, \tag{23}$$

$$P_8 = \pm\sqrt{-\frac{b}{C_2}}\left(\frac{-6C_1b\operatorname{csch}^2(\sqrt{-C_1}\eta)}{3b^2+4C_1c(1+\varepsilon\coth(\sqrt{-C_1}\eta))^2}\right)^{\frac{1}{2}}, \quad C_1 < 0, C_3 = \frac{-C_2^2c}{b^2}, d = 0, \tag{24}$$

$$P_9 = \pm\sqrt{-\frac{b}{C_2}}\left(\frac{6C_1\operatorname{sech}^2(\sqrt{-C_1}\eta)}{3b+4\sqrt{-3C_1c}\tanh(\sqrt{-C_1}\eta)}\right)^{\frac{1}{2}}, \quad C_1 < 0, C_3 = \frac{-C_2^2c}{b^2}, d = 0, \tag{25}$$

$$P_{10} = \pm\sqrt{-\frac{b}{C_2}}\left(\frac{-6C_1\operatorname{csch}^2(\sqrt{-C_1}\eta)}{3b+4\sqrt{-3C_1c}\coth(\sqrt{-C_1}\eta)}\right)^{\frac{1}{2}}, \quad C_1 < 0, C_3 = \frac{-C_2^2c}{b^2}, d = 0, \tag{26}$$

$$P_{11} = \pm\sqrt{-\frac{b}{C_2}}\left(\frac{6C_1\sec^2(\sqrt{C_1}\eta)}{3b+4\sqrt{3C_1c}\tan(\sqrt{C_1}\eta)}\right)^{\frac{1}{2}}, \quad C_1 > 0, C_3 = \frac{-C_2^2c}{b^2}, d = 0, \tag{27}$$

$$P_{12} = \pm\sqrt{-\frac{b}{C_2}}\left(\frac{6C_1\csc^2(\sqrt{C_1}\eta)}{3b+4\sqrt{3C_1c}\cot(\sqrt{C_1}\eta)}\right)^{\frac{1}{2}}, \quad C_1 > 0, C_3 = \frac{-C_2^2c}{b^2}, d = 0, \tag{28}$$

$$P_{13} = \pm 2\sqrt{-\frac{b}{C_2}}\left(\frac{-3C_1\operatorname{sech}^2(\varepsilon\sqrt{-C_1}\eta)}{2\sqrt{M}-(\sqrt{M}+3b)\operatorname{sech}^2(\varepsilon\sqrt{-C_1}\eta)}\right)^{\frac{1}{2}} \quad C_1 < 0, C_3 = \frac{-C_2^2c}{b^2}, d = 0, \tag{29}$$

$$P_{14} = \pm 2\sqrt{-\frac{b}{C_2}}\left(\frac{-3C_1\operatorname{csch}^2(\varepsilon\sqrt{-C_1}\eta)}{2\sqrt{M}+(\sqrt{M}-3b)\operatorname{csch}^2(\varepsilon\sqrt{-C_1}\eta)}\right)^{\frac{1}{2}}C_1 < 0, \quad C_3 = \frac{-C_2^2c}{b^2}, d = 0, \tag{30}$$

$$P_{15} = \pm 2\sqrt{-\frac{b}{C_2}}\left(\frac{3C_1\sec^2(\varepsilon\sqrt{C_1}\eta)}{2\sqrt{M}-(\sqrt{M}-3b)\sec^2(\varepsilon\sqrt{C_1}\eta)}\right)^{\frac{1}{2}} \quad C_1 > 0, C_3 = \frac{-C_2^2c}{b^2}, d = 0, \tag{31}$$

$$P_{16} = \pm 2\sqrt{-\frac{b}{C_2}}\left(\frac{-3C_1\csc^2(\varepsilon\sqrt{C_1}\eta)}{2\sqrt{M}-(\sqrt{M}+3b)\csc^2(\varepsilon\sqrt{C_1}\eta)}\right)^{\frac{1}{2}} \quad C_1 > 0, C_3 = \frac{-C_2^2c}{b^2}, d = 0, \tag{32}$$

$$P_{17} = \pm 2\sqrt{-\frac{b}{C_2}}\left(\frac{-3C_1}{\varepsilon\sqrt{M}\cosh(2\sqrt{-C_1}\eta)-3b}\right)^{\frac{1}{2}} \quad C_1 > 0, C_3 = \frac{-C_2^2c}{b^2}, d = 0, \tag{33}$$

$$P_{18} = \pm 2\sqrt{-\frac{b}{C_2}}\left(\frac{-3C_1}{\varepsilon\sqrt{M}\cos(2\sqrt{C_1}\eta)-3b}\right)^{\frac{1}{2}} \quad C_1 > 0, C_3 = \frac{-C_2^2c}{b^2}, d = 0, \tag{34}$$

$$P_{19} = \pm 2\sqrt{-\frac{b}{C_2}}\left(\frac{-3C_1}{\varepsilon\sqrt{M}\sin(2\sqrt{C_1}\eta)-3b}\right)^{\frac{1}{2}} \quad C_1 > 0, C_3 = \frac{-C_2^2c}{b^2}, d = 0, \tag{35}$$

$$P_{20} = \pm 2\sqrt{-\frac{b}{C_2}}\left(\frac{-3C_1}{\varepsilon\sqrt{-M}\sinh(2\sqrt{-C_1}\eta)-3b}\right)^{\frac{1}{2}} \quad C_1 > 0, C_3 = \frac{-C_2^2c}{b^2}, d = 0, \tag{36}$$

where $M = 6b^2 + 48C_1c$, $\varepsilon = \pm 1$. Through back-substitution of the relation provided by Eq. (13) in Eq. (4), numerous novel chirped solitary waves, ψ_i, $i = 1, \ldots, 20$, are discovered for the VCQNLE.

4 Physical applications

Chirp waves, whose frequency changes over time, and solitons, self-reinforcing solitary waves, have a complex interplay. Chirp waves can compress solitons, generate new ones, and influence their dynamics [32]. This interaction

is crucial in various fields, including optical communications, nonlinear optics, and plasma physics. By understanding and controlling chirp wave-soliton interactions, researchers can advance technologies such as high-speed data transmission, laser systems, and plasma-based energy generation [33–35]. We calculate the chirp for our problem using the following equation:

$$\delta\omega = -\frac{\partial}{\partial t}(r(x) - qt + f(\eta)). \tag{37}$$

From Eq. (10),

$$\delta\omega(x,t) = \frac{\delta(x)}{2\alpha(x)}P^2 - \frac{k}{2\alpha(x)}. \tag{38}$$

Using P_1 and P_2 as examples, we can calculate the chirp using the following formula:

$$\delta\omega_1(x,t) = -\frac{8C_1\delta(x)}{3C_2\alpha(x)}\left(\frac{\tanh^2\left(\varepsilon\sqrt{\frac{C_1}{3}}\eta\right)}{3+\tanh^2\left(\varepsilon\sqrt{\frac{C_1}{3}}\eta\right)}\right) - \frac{k}{2\alpha(x)}. \tag{39}$$

$$\delta\omega_2(x,t) = -\frac{C_1\delta(x)}{C_2\alpha(x)}\left(1+\tanh^2\left(\varepsilon\sqrt{\frac{C_1}{3}}\eta\right)\right) - \frac{k}{2\alpha(x)}. \tag{40}$$

4.1 Dynamic behavior of solutions

Nonuniform management system refers to a system where the control parameters are not uniform, leading to a more complex and realistic scenario. Therefore, this variability in the VCQNLE coefficients allows it to effectively model the dynamics of nonuniform management systems [11]. By mapping the parameters of the management system to the VCQNLE, we can use the equation to present more complicated phenomena in optics and plasma physics [3–5]. According to that, we will now concentrate on how specific parameters influence wave propagation, drawing primarily from Eqs (39) and (13). Of these, only two parameters significantly impact wave propagation: the group velocity $\alpha(x)$ and the Raman effect $\delta(x)$. Given that the Raman parameter marks the quintic term in the VCQNLE, we will focus our attention on its effects. Therefore, we have set the following constant values for all figures: $C_1 = 2$, $C_2 = 3$, $\varepsilon = 1$, $k = 0.5$, where $C_1 = -2$ in figures (b), we will vary the values of $\alpha(x)$ and $\delta(x)$ as specified.

Case I: To isolate the effects of $\alpha(x)$ and $\delta(x)$, we will set them to have equal magnitudes. In Figure 1(a) and (b), $\delta(x) = \alpha(x) = 0.25$, but in Figure 2(a) and (b), it takes $\delta(x) = -0.25$, $\alpha(x) = 0.25$.

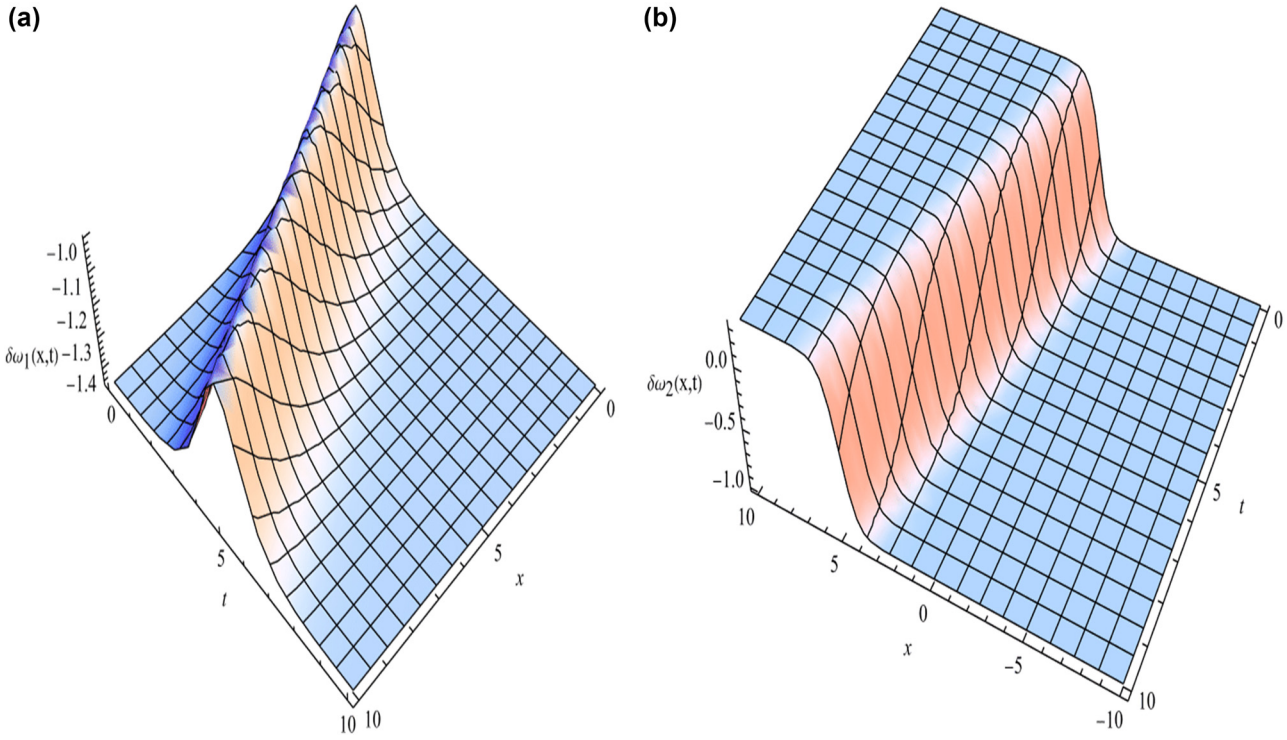

Figure 1: The 3D plot of the bright soliton $\delta\omega_1$ and the kink wave $\delta\omega_2$ given by Eqs (39) and (40), which describe ultrashort optical pulses in nonlinear optics. (a) The bright soliton wave $\delta\omega_1$ and (b) the kink wave $\delta\omega_2$.

In Figure 1(a) and (b), it is clear that in the case of nonlinearity management system where the GVD is taken as a constant value $\alpha(x) = 0.25$, the chirp wave becomes as a bright soliton $\delta(x) = 0.25$ in Figure 1(a) and becomes a dark soliton when the sign of the Raman effect changes to negative $\delta(x) = -0.25$ in Figure 2(a), but this does not affect the kink wave in Figures 1(b) and 2(b). In Figures 3(a) and 4(a), we can see that when the GVD is fixed as $\alpha(x) = e^{3x}$ and $\delta(x) = \pm e^{2x}$, it makes the amplitude of the chirp wave $\left|-\frac{8C_1\delta(x)}{3C_2\alpha(x)}\right| = \frac{8}{9}e^{-x}$, which is responsible for the oscillations. Moreover, in both Figures 3(a) and 4(a), the chirp wave takes a parabolic shape affected by the choices of the exponential functions in both $\alpha(x)$ and $\delta(x)$. On the other hand, the kink-like chirp wave solution $\delta\omega_2$ in Figures 3(b) and 4(b) is affected by the variable amplitude $\left|-\frac{C_1\delta(x)}{C_2\alpha(x)}\right| = \frac{2}{3}e^{-x}$ and have a parabolic shape.

4.2 Solution stability

The motion of conservative systems in classical mechanics is described by the Hamiltonian system. The momentum is given as [10]

$$m = \lim_{s\to\infty}\int_0^s |\psi(x,t)|_l^2 \mathrm{d}x, \tag{41}$$

where $l = 1, 2, 3, \ldots, 20$. The solution's $\psi_1, \ldots, \psi_{20}$ stability conditions are satisfied if

$$\frac{\partial m}{\partial k} > 0. \tag{42}$$

If we take $\psi_1(x,t)$ as instant to apply stability

$$|\psi_1(x,t)|^2 = 4\left(-\frac{b}{C_2}\right)\frac{C_1\tanh^2\left(\varepsilon\sqrt{\frac{C_1}{3}}(t-kx)\right)}{3b\left(3+\tanh^2\left(\varepsilon\sqrt{\frac{C_1}{3}}(t-kx)\right)\right)},$$

$$C_1 > 0, b > 0, C_3 = \frac{3C_2^2}{16C_1}.$$

Therefore, the important conditions for the solitary wave solution ψ_1 to be stable are

$$C_1 > 0, \quad b > 0, \quad C_3 = \frac{3C_2^2}{16C_1}, \quad C_2 < 0. \tag{43}$$

5 Conclusion

Using mapping method combined with variable chirp wave transformation (4), we have successfully constructed different types of chirp wave solutions including bright soliton, dark soliton solutions, kink shaped profiles, and singular periodic solutions of the VCQNLE. We have

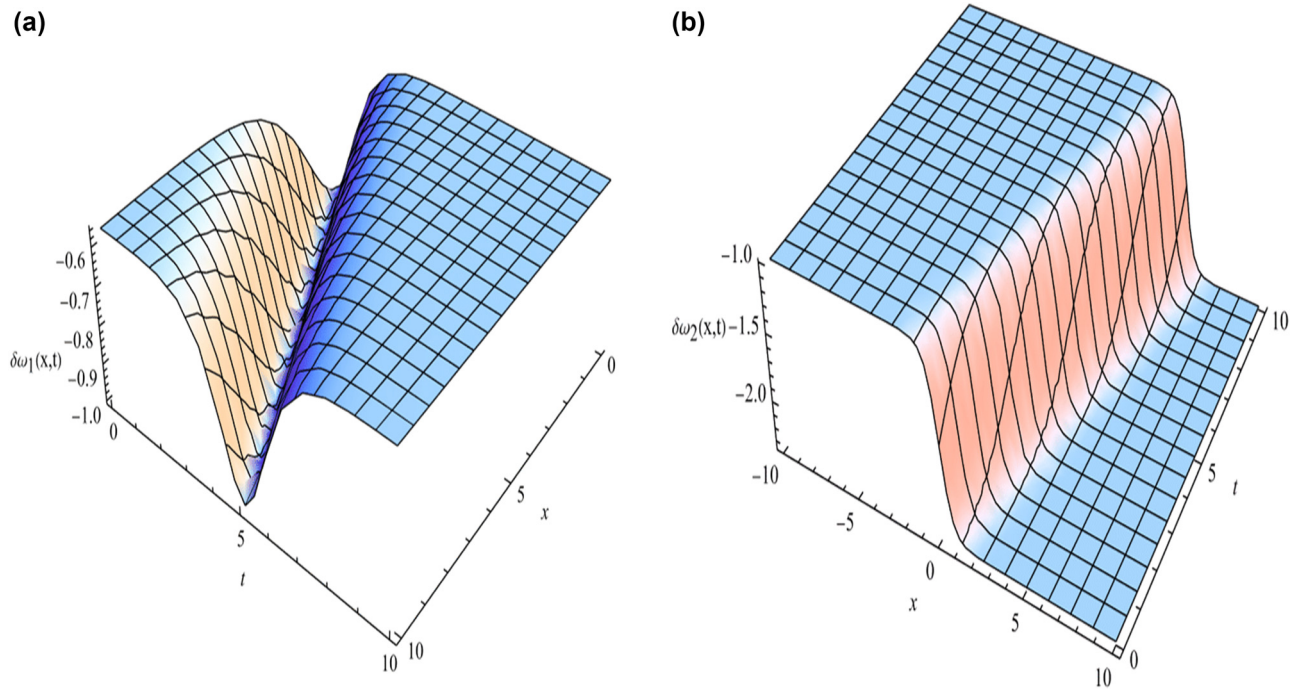

Figure 2: The 3D plot of the dark chirp soliton solution $\delta\omega_1$ and the kink chirp wave $\delta\omega_2$ given by Eqs (39) and (40), which can describe ultrashort optical pulses in nonlinear optics. (a) The dark chirp wave and (b) the kink chirp wave.

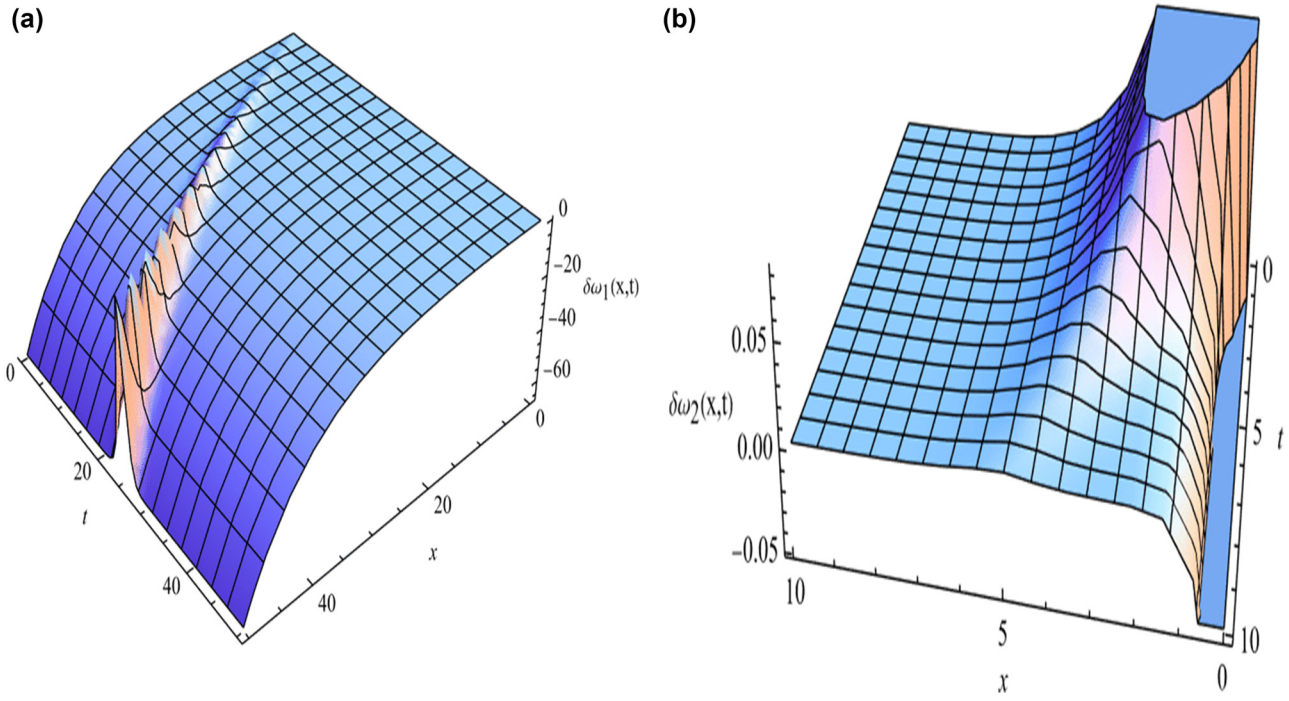

Figure 3: The evolution 3D plot of the bright soliton chirp wave $\delta\omega_1$ and kink chirp wave $\delta\omega_2$ in the exponential distributed fiber when the GVD is fixed as $\alpha(x) = e^{3x}$ and the variable Raman effect $\delta(x) = e^{2x}$. (a) The bright soliton $\delta\omega_1$ in the exponential distributed fiber and (b) the kink chirp wave $\delta\omega_2$ in the exponential distributed fiber.

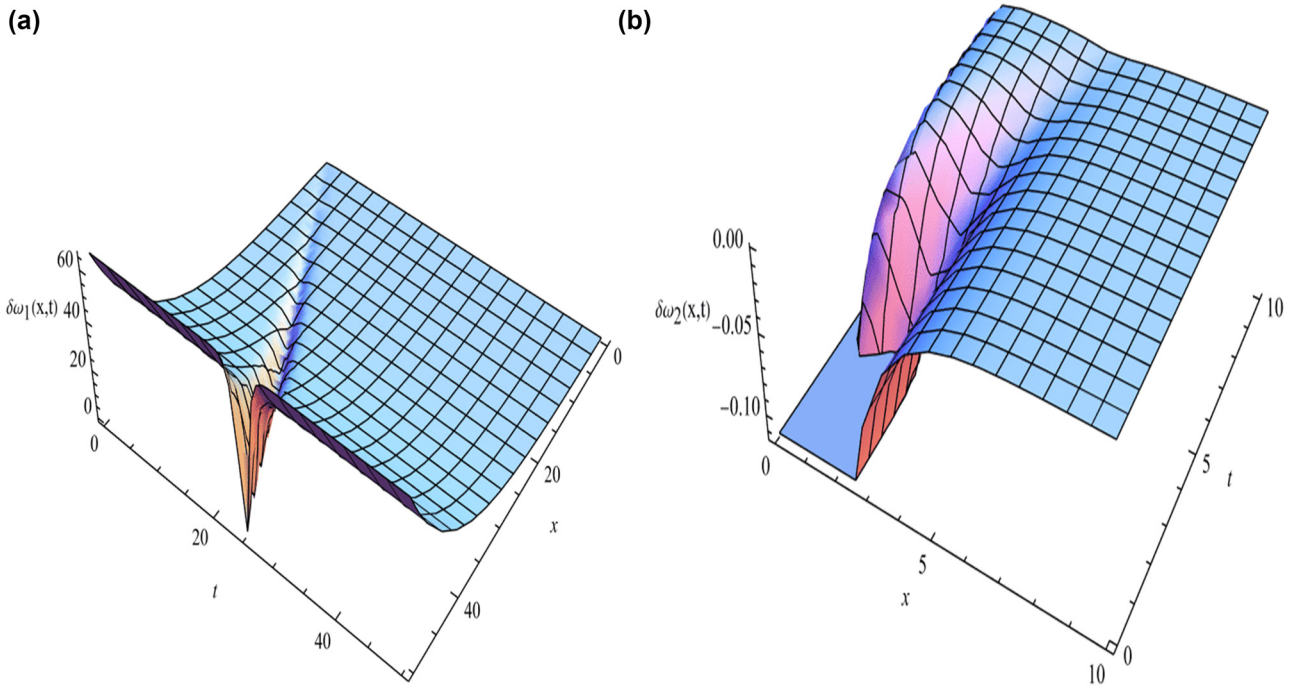

Figure 4: The 3D plot of the dark soliton chirp wave $\delta\omega_1$ and the kink chirp wave $\delta\omega_2$ in the exponential distributed fiber when the GVD is fixed as $\alpha(x) = e^{3x}$ and the variable Raman effect $\delta(x) = e^{2x}$. (a) The dark soliton $\delta\omega_1$ in the exponential distributed fiber and (b) the kink chirp wave $\delta\omega_2$ in the exponential distributed fiber.

provided graphical and physical explanations by creating 3D diagrams, illustrating how the variables GVD $\alpha(x)$ and Raman effect $\delta(x)$ controlled the dynamic behavior of the wave solutions propagation. Following are the important concluding remarks:

1) Compared with other studies before the VCQNLE [12–18], the obtained chirp wave solutions cover other solutions in the literature and contain new ones.
2) The utilization of these obtained solutions shows simplicity, effectiveness, and power of the mapping method.
3) The visualization of the soliton and kink chirp waves shows that their shape can be changed by controlling the GVD $\alpha(x)$ and Raman effect $\delta(x)$, whereby changing the two variable functions from constant case I to the variable exponential case II, the shape is affected in the second case and oscillations appear because of the inhomogeneity of the coefficients.
4) When we have fixed the value of $\alpha(x)$ and change the sign of $\delta(x)$ in Figures 1(a) and 2(a) as positive and negative, respectively, the chirp wave changes from bright to dark soliton. Similarly in Figures 3(a) and 4(a), the sign of the Raman effect $\delta(x)$ changes the soliton shape from bright (positive sign) to dark soliton (negative sign) but does not affect the kink chirp.
5) The stability of the obtained solutions was studied for $\psi_1(x, t)$ and the necessary conditions were found, and in the same way, we can construct for other solutions.
6) The obtained solutions can have many applications in optic fiber communications and plasma physics.

Since, it was the first time to apply mapping method on variable coefficient equations like VCQNLE, we hope to use it in the future studies with other variable coefficients evolution equations.

Acknowledgments: The authors would like to thank the Deanship of Scientific Research, Majmaah University, Saudi Arabia, for funding this work under project Number R-2025-1688.

Funding information: This work was funded by the Deanship of Scientific Research, Majmaah University, Saudi Arabia under project Number R-2025-1688.

Author contributions: All authors have accepted responsibility for the entire content of this manuscript and approved its submission.

Conflict of interest: The authors state no conflict of interest.

Data availability statement: All data generated or analysed during this study are included in this published article.

References

[1] Raza N, Hassan Z, Seadawy A. Computational soliton solutions for the variable coefficient nonlinear Schrödinger equation by collective variable method. Opt Quantum Electron. 2021;53:1–16. doi: 10.1007/S11082-021-03052-1/FIGURES/2.

[2] Nchejane JN, Gbenro SO. Nonlinear Schrödinger equations with variable coefficients: numerical integration. J Adv Math Comput Sci. 2022;37:56–69. doi: 10.9734/JAMCS/2022/v37i330442.

[3] Chen SS, Tian B, Qu QX, Li H, Sun Y, Du XX. Alfvén solitons and generalized Darboux transformation for a variable-coefficient derivative nonlinear Schrödinger equation in an inhomogeneous plasma. Chaos Solitons Fractals. 2021;148:111029. doi: 10.1016/J.CHAOS.2021.111029.

[4] González-Gaxiola O, Biswas A, Alzahrani AK, Belic MR. Highly dispersive optical solitons with a polynomial law of refractive index by Laplace-Adomian decomposition. J Comput Electron. 2021;20:1216–23. doi: 10.1007/S10825-021-01710-X/FIGURES/6.

[5] Xu SL, Petrović N, Belić MR, Deng W. Exact solutions for the quintic nonlinear Schrödinger equation with time and space. Nonlinear Dyn. 2016;84:251–9. doi: 10.1007/S11071-015-2426-1/FIGURES/8.

[6] Dai C, Wang Y, Yan C. Chirped and chirp-free self-similar cnoidal and solitary wave solutions of the cubic-quintic nonlinear Schrödinger equation with distributed coefficients. Opt Commun. 2010;283:1489–94. doi: 10.1016/J.OPTCOM.2009.11.082.

[7] El-Shiekh RM, Gaballah M. Novel solitary and periodic waves for the extended cubic (3+1)-dimensional Schrödinger equation. Opt Quantum Electron 2023;55:1–12. doi: 10.1007/S11082-023-04965-9/METRICS.

[8] El-Shiekh RM, Gaballah M. Solitary wave solutions for the variable-coefficient coupled nonlinear Schrödinger equations and Davey-Stewartson system using modified sine-Gordon equation method. J Ocean Eng Sci. 2020;5:180–5. doi: 10.1016/J.JOES.2019.10.003.

[9] El-Shiekh RM, Gaballah M. New rogon waves for the nonautonomous variable coefficients Schrödinger equation. Opt Quantum Electron. 2021;53:1–12. doi: 10.1007/S11082-021-03066-9/FIGURES/3.

[10] Gaballah M, El-Shiekh RM. Novel picosecond wave solutions and soliton control for a higher-order nonlinear Schrödinger equation with variable coefficient. Alexandria Eng. J 2025;114:419–25. doi: 10.1016/J.AEJ.2024.11.078.

[11] Wang P, Feng L, Shang T, Guo L, Cheng G, Du Y. Analytical soliton solutions for the cubic-quintic nonlinear Schrödinger equation with Raman effect in the nonuniform management systems. Nonlinear Dyn. 2015;79:387–95. doi: 10.1007/S11071-014-1672-Y/FIGURES/9.

[12] Xie XY, Yan ZH. Soliton collisions for the Kundu-Eckhaus equation with variable coefficients in an optical fiber. Appl Math Lett. 2018;80:48–53. doi: 10.1016/J.AML.2018.01.003.

[13] Baylndlr C. Rogue wave spectra of the Kundu-Eckhaus equation. Phys Rev E. 2016;93:062215. doi: 10.1103/PHYSREVE.93.062215/FIGURES/9/MEDIUM.

[14] Mirzazadeh M, Yıldırım Y, Yaşar E, Triki H, Zhou Q, Moshokoa SP, et al. Optical solitons and conservation law of Kundu-Eckhaus equation. Optik (Stuttg). 2018;154:551–7. doi: 10.1016/J.IJLEO.2017.10.084.
[15] Kumar D, Manafian J, Hawlader F, Ranjbaran A. New closed form soliton and other solutions of the Kundu-Eckhaus equation via the extended sinh-Gordon equation expansion method. Optik (Stuttg) 2018;160:159–67. doi: 10.1016/J.IJLEO.2018.01.137.
[16] El-Borai MM, El-Owaidy HM, Ahmed HM, Arnous AH, Moshokoa S, Biswas A, et al. Topological and singular soliton solution to Kundu-Eckhaus equation with extended Kudryashov's method. Optik (Stuttg). 2017;128:57–62. doi: 10.1016/J.IJLEO.2016.10.011.
[17] Rezazadeh H, Korkmaz A, Eslami M, Mirhosseini-Alizamini SM. A large family of optical solutions to Kundu-Eckhaus model by a new auxiliary equation method. Opt Quantum Electron. 2019;51:1–12. doi: 10.1007/S11082-019-1801-4/METRICS.
[18] Xie XY, Tian B, Sun WR, Sun Y. Rogue-wave solutions for the Kundu-Eckhaus equation with variable coefficients in an optical fiber. Nonlinear Dyn. 2015;81:1349–54. doi: 10.1007/S11071-015-2073-6/FIGURES/2.
[19] Wang DS, Guo B, Wang X. Long-time asymptotics of the focusing Kundu-Eckhaus equation with nonzero boundary conditions. J Differ Equ. 2019;266:5209–53. doi: 10.1016/J.JDE.2018.10.053.
[20] Wang X, Yang B, Chen Y, Yang Y. Higher-order rogue wave solutions of the Kundu-Eckhaus equation. Phys Scr. 2014;89:095210. doi: 10.1088/0031-8949/89/9/095210.
[21] Baskonus HM, Bulut H. On the complex structures of Kundu-Eckhaus equation via improved Bernoulli sub-equation function method. Waves Random Complex Media. 2015;25:720–8. doi: 10.1080/17455030.2015.1080392.
[22] Islam SMR, Ahmad H, Khan K, Wang H, Akbar MA, Awwad FA, et al. Stability analysis, phase plane analysis, and isolated soliton solution to the LGH equation in mathematical physics. Open Phys. 2023;21:20230104. doi: 10.1515/PHYS-2023-0104/ASSET/GRAPHIC/J_PHYS-2023-0104_FIG._008.JPG.
[23] El-Shiekh RM, Gaballah M. Ultrashort chirp pulses for Kundu-Eckhaus equation in nonlinear optics. Opt Quantum Electron. 2024;56:1–10. doi: 10.1007/S11082-024-07222-9/METRICS.
[24] Triki H, Sun Y, Biswas A, Zhou Q, Yıldırım Y, Zhong Y, et al. On the existence of chirped algebraic solitary waves in optical fibers governed by Kundu-Eckhaus equation. Results Phys. 2022;34:105272. doi: 10.1016/J.RINP.2022.105272.
[25] Daoui AK, Messouber A, Triki H, Zhou Q, Biswas A, Liu W, et al. Propagation of chirped periodic and localized waves with higher-order effects through optical fibers. Chaos Solitons Fractals. 2021;146:110873. doi: 10.1016/J.CHAOS.2021.110873.
[26] Zayed EME, Alurrfi KAE. Solitons and other solutions for two nonlinear Schrödinger equations using the new mapping method. Optik (Stuttg). 2017;144:132–48. doi: 10.1016/J.IJLEO.2017.06.101.
[27] Zayed EME, Alurrfi KAE, Alshbear RA. On application of the new mapping method to magneto-optic waveguides having Kudryashov's law of refractive index. Optik (Stuttg). 2023;287:171072. doi: 10.1016/J.IJLEO.2023.171072.
[28] Zayed EME, Alngar MEM, Shohib RMA, Biswas A, Yıldırım Y, Alshomrani AS, et al. Optical solitons having Kudryashov's self-phase modulation with multiplicative white noise via Itô Calculus using new mapping approach. Optik (Stuttg). 2022;264:169369. doi: 10.1016/J.IJLEO.2022.169369.
[29] Islam SMR, Arafat SMY, Alotaibi H, Inc M. Some optical soliton solution with bifurcation analysis of the paraxial nonlinear Schrödinger equation. Opt Quantum Electron. 2024;56:1–16. doi: 10.1007/S11082-023-05783-9/METRICS.
[30] Islam SMR, Basak US. On traveling wave solutions with bifurcation analysis for the nonlinear potential Kadomtsev-Petviashvili and Calogero-Degasperis equations. Partial Differ Equations Appl Math. 2023;8:100561. doi: 10.1016/J.PADIFF.2023.100561.
[31] Islam SMR, Khan K, Akbar MA. Optical soliton solutions, bifurcation, and stability analysis of the Chen-Lee-Liu model. Results Phys. 2023;51:106620. doi: 10.1016/J.RINP.2023.106620.
[32] Spiess C, Yang Q, Dong X, Renninger WH, Bucklew VG. Chirped dissipative solitons in driven optical resonators. Opt 2021;8(6):861– 9. doi: 10.1364/OPTICA.419771.
[33] Kivshar Y, Agrawal G. Optical solitons: from fibers to photonic crystals. New York: Academic Press; 2003.
[34] Mandeng LM, Tchawoua C, Tagwo H, Zghal M, Cherif I, Mohamadou A. Role of the input profile asymmetry and the Chirp on the propagation in highly dispersive and nonlinear fibers. J Light Technol 2016;34:5635–41. doi: 10.1109/JLT.2016.2624699.
[35] Cai W, Yang Z, Wu H, Wang L, Zhang J, Zhang L, et al. Effect of chirp on pulse reflection and refraction at a moving temporal boundary. Opt Express. 2022;30:34875–86. doi: 10.1364/OE.462333.